Evaluation of the Corrosion Behavior of Inconel 625 Superalloy Made by SLM Method

Lamyaa Idkhayyil Mahood A.[1], M. Razazi Boroujeni[2,*]

[1]Department of Materials Engineering, South Tehran Branch, Islamic Azad University, Tehran, Iran.
[2]Department of Materials Engineering, Lenjan Branch, Islamic Azad University, Isfahan, Iran.
Received: 02 May 2024 - Accepted: 28 November 2024

Abstract

The purpose of this research is to investigate the corrosion resistance of Inconel 625 alloy produced by selective laser melting after heat treatment and surface treatment. For this purpose, the samples produced with the help of a Selective Laser Melting Machine (SLM) were prepared in four modes of the prototype (without further treatment), heat treated, surface treated, and finally heat treatment and consecutive surface treatment. To perform heat treatment, the combined cycle of annealing and aging was used. In the surface treatment, the shot pinning method was used for 30 minutes using steel balls. X-ray diffraction analysis was performed to determine the phase of the samples. Peaks of the primary γphase, nickel carbide, and molybdenum were revealed in the heat-treated samples. In the following, the samples were electrochemically evaluated in 3.5 wt.% NaCl medium with potentiodynamic polarization tests and Electrochemical Impedance Spectroscopy (EIS). The results showed that the SLM-HT sample has the most positive corrosion potential and the lowest corrosion current density, while the SLM 625 sample shows the most negative corrosion potential and the highest corrosion current density. Heat treatment improved both thermodynamic behavior and kinetic behavior, but the surface treatment had little effect on improving corrosion. Also, the results of the EIS test showed that the HT-625 sample had the highest polarization resistance and the lowest charge accumulation (capacitance),while the 625 sample showed the lowest charge transfer/polarization resistance and the highest capacitance.

Keywords: Heat Treatment, Inconel 625, Selective Laser Melting, Corrosion.

1. Introduction

Inconel 625 is a nickel-based austenitic superalloy. Due to the favorable properties that this alloy has at temperatures between ultra-cold temperatures (temperatures within a few degrees of absolute zero) and temperatures of 1800 degrees Fahrenheit (1255 K), it is used in a wide variety of applications (e.g., aviation, aerospace, chemical, petrochemical, marine). The initial design of Inconel 625 alloy is a combination of desirable properties, including high tensile strength, high creep and tear resistance, high fracture toughness, good weldability, and low and high-temperature corrosion resistance [1].

Although Inconel 625 was originally designed as a solid solution reinforced with molybdenum and niobium, it soon became clear that aging and precipitation hardness have been added to its strengthening and hardening mechanism. This unique combination of properties makes Inconel 625 alloy very versatile. Like most nickel-based superalloys, the main phase in Inconel 625 is the nickel austenitic phase, gama (γ), which forms a Face-Centered Cubic matrix (FCC) [1].

The gamma phase is rich in substitution solid-solution alloying elements of chromium, molybdenum, niobium, and iron substitution, which are commonly known as gamma phase builders and constituents [1].unlike subtractive manufacturing, AM processes offer the ability to manufacture metal components with complex geometries without wasting existing materials such as geometries that cannot be achieved using conventional manufacturing techniques. In addition, additive manufacturing enables the easy creation of custom designs and prototypes.

This reduces the cost of tooling and subsequent additional operations such as machining, etc., resulting in a cost-effective way to produce parts[2].

In contrast, metals produced by AM can contain defects directly related to the manufacturing process, including porosity, lack of fusion, and internal stresses.

Likewise, rapid cooling rates during solidification can lead to the segregation of alloying elements and harmful phases in the metal. To minimize process-related defects, heat treatment (for example, stress relief, isostatic hot pressing, and solution treatment) is generally performed after the fabrication of additively manufactured metal parts [3].

In these years, several research have been conducted on the effect of heat treatment and also surface treatment on the mechanical and corrosion behavior of Inconel 625 alloy, but this is the first time in this research that the effect of simultaneous application of heat treatment and surface treatment on the corrosion resistance of this alloy has been investigated.

[*]Corresponding author
Email address: mohamad.razazi@yahoo.com

2. Materials and Methods

Spherical plasma atomized powder of IN625 alloy was purchased. The size of the powders was in the range of 25 to 40 micrometers. Selective laser melting machine (SLM) Nora model was used to produce the samples. Cylindrical samples with a diameter of 8 mm and a height of 12 mm were made and 3 repetitions were considered for each test condition. The printed samples were evaluated in as-built (SLM 625), heat-treated (HT), surface-treated (ST), heat-treated and surface-treated (HT-ST) states. For heat treatment, solution annealing was done at 1000°C for 1 hour and then they were completely cooled with air. In order to carry out aging heat treatment, the samples were placed at a temperature of 700 degrees Celsius for 16 hours. The shot pinning method was used for the surface treatment of SLM samples. To investigate phase changes and detect possible new phases, X-ray diffraction analysis was performed with a Philips XPERT-MPD device and CuKα radiation. High Score Plus version 3.0.5 software was used for phase detection. The corrosion behavior of the samples was investigated with the help of the cyclic potentiodynamic polarization test and electrochemical impedance spectroscopy.

3. Results and Discussion

3.1. Phase Analysis

In order to identify the phases present in different samples, XRD analysis was performed. Fig. 1. shows the XRD patterns of all four samples in the range of 20-100 degrees. As it is known, in SLM 625 and SLM 718-ST samples, the primary γ phase peaks (FeNi with ICOD 00-003-1209 and cubic crystal structure) while for SLM 718-HT and SLM 718-HT-ST samples Primary γ phase, nickel carbide (Ni_3C_{36} with COD 960407-3522 and hexagonal crystal structure) and molybdenum (Mo with COD 96-900-8475 and cubic crystal structure) have been detected.

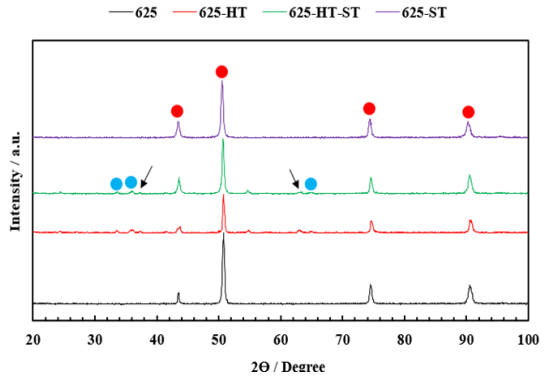

Fig. 1. XRD patterns of different samples in the range of 2Θ = 20-90° with a scan rate of 0.05°/s.

Laves phases in 625 and 625-ST and δ phase in 625-HT and 625-HT-ST samples could not be detected by XRD peaks. In the XRD pattern, the red circle is the austenite phase, the blue circle is the nickel carbide, and the arrow is the molybdenum phase [4].

3.2Polarization Test

In this research, the corrosion and electrochemical behavior of SLM Inconel 625 was investigated in four different states: raw (code 625), heat treated (code 625-HT), surface treatment through shot-peened for a specified period of 1 hour (code 625-ST), and the mixture of surface and heat treatment (code 625-ST-HT). The SLM samples (four modes) were exposed to electrochemical tests using the Ivium device made in the Netherlands according to the ASTM-G59 standard (standard test method for measuring potentiodynamic polarization resistance). In general, electrochemical tests (potentiodynamic polarization and electrochemical impedance spectroscopy) were performed in a 3-electrode cell. The sample was used as a working electrode (WE), Ag/AgCl electrode (KCl Saturated) as reference electrode (RE), and platinum as the counter electrode (CE).The heat treatment cycle performed on the Inconel 625 sample made by the selective laser melting method was chosen in such a way that the sample was first dissolved and annealed at 1000°C for 1 hour, then rapidly cooled (cooling in water), then two stages of aging were done separately at 700 and 600 degrees Celsius, respectively.The interval between two hard aging stages which were at a very slow rate (in the oven) is about 3 hours.The potentiodynamic polarization test was conducted to evaluate the corrosion resistance of different SLM samples.

First, the samples were placed in 3.5 wt.% NaCl solution for 3600 seconds (1 hour) under open circuit conditions (OCP) to reach steady state conditions. In all cases, the potential moved from the initial state to more positive values, which indicates the formation of an oxide film on the surface of the samples and finally stabilization.

After reaching stable conditions, the polarization test was performed in the range of 250 mV lower than OCP and 1.5 V absolute with a scan rate of 1 mV/s. Fig. 2. shows the potentiodynamic polarization curves of all four samples.

The cyclic potentiodynamic polarization test was performed on the samples. The reversible potential was chosen to be +0.85 V, because the Tafel test was performed on the raw SLM sample before the cycle test. The Tafel diagram showed that in the range of +0.8 V and above, the intensity of the increase in current density is significantly higher than before. This point can be considered as a possible failure potential. Generally, due to the corrosion of metal M, metal cations M^{z+} are produced and enter the solution.

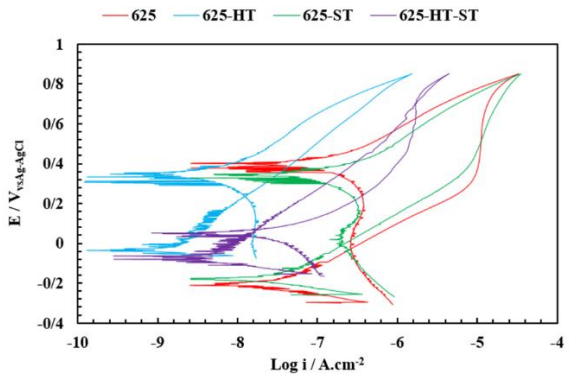

Fig. 2. Potentiodynamic polarization curves of Inconel 625 SLM samples in different states in 3.5 wt.% NaCl solution at room temperature.

In the Evans or polarization diagram, active region is detected. At a critical point, when the concentration of M^{z+} ions reaches a certain level, the ability to form the passive layer is provided. In other words, the driving force necessary for passivationis provided in the critical current density (i_{crit}). At this current density, oxide/hydroxidegermes are formed on the metal surface. Then these germes grow, join together and create a protective layer on the surface of the metal. It is noteworthy that the higher the i_{crit} for an alloy, the weaker the corrosion resistance of that material.

In such a way that sometimes passivationis not useful. It can be said that the layer formed on the surface at a lower i_{crit} acts as a barrier layer, while the layer formed at a higher i_{crit} acts as a physical barrier. Barrier layer is a strong, sticky and defect-free layer, while the physical layer is a loose, vacancy-filled layer. The primary potential of passivation is shown with the symbol E_{pp} (primary passive). With the formation of the upper layer, the corrosion rate of M metal is greatly reduced and reaches a certain value.

In a potential range, the passive layer remains stable. In the Evans diagram, this range is called the passive region. With the increase of the potential, passive layer breaks down and disappears. Metal corrosion becomes severe again. After the breakdown potential (destruction point), the material enters the transpassive region [5].

Cathodic branch of cyclic potentiodynamic polarization curves for all four samples shows similar behavior. In fact, the type and mechanism of the cathodic/ambient reaction are the same. The analysis of the anode branch is as follows:

All four samples are actively corroded. In fact, only the active area is observed. The slope of the active area is similar for SLM and SLM-ST samples, while they are different from the same slope of SLM-HT and SLM-HT-ST samples.

This slope difference is indicative of the change in the corrosion mechanism of the sample in the corrosive environment. Two samples SLM and SLM-ST have an almost constant current density at high current density in a high potential range.

Due to the high current density, the layer formed on the two samples is known as a physical barrier.

Upon reaching the reversible potential, all the samples returned from the back (left side of the curve), which means that they are resistant to pitting. The reason is the presence of Mo in the chemical composition of the alloy in a large amount of 8-10%. Many mechanisms have been proposed to increase pitting resistance, including:

- The active areas are coated with molybdenum oxyhydroxide or molybdate salts, thereby preventing local attack.
- The dissolution of Mo in the alloy produces molybdate ions, which will then act as a corrosion inhibitor near the metal surface.
- Mo^{6+} species in the coating film react with cationic vacancies of opposite sign and reduce the flux of cationic vacancies to the metal substrate.
- Molybdate ions act as a cation-selective outer layer in the passive film and thus delay the transport of Cl^- ions through the passive film.
- Molybdenum participates with active dissolution kinetics at the base of the cavity being created [6].

In Table. 1., the information extracted from the cyclic potentiodynamic polarization diagrams for all samples is reported separately.

Table. 1. Values of potential and corrosion current density extrapolated from the Tafel region (non-linear region) of E-logi curves for different samples.

Parameter	SLM-HT-ST	SLM-ST	SLM-HT	SLM
E_{corr} (V)	- 0.093	- 0.18	- 0.015	- 0.21
i_{corr}(A.cm^{-2})	5.01 × 10^{-9}	1.05 × 10^{-8}	1.58 × 10^{-9}	1.58 × 10-8

Based on Fig. 1. and the data in Table. 1., the SLM-HT sample has the most positive corrosion potential and the lowest corrosion current density, while the SLM 625 sample shows the most negative corrosion potential and the highest corrosion current density. Corrosion potential represents the thermodynamic behavior and i_{Corr} represents the kinetic behavior of the sample. Therefore, heat treatment improves both the thermodynamic behavior and the kinetic behavior of the SLM 625 sample against corrosion. Since heat treatment affects the microstructure and corrosion resistance of Inconel 625 made by selective laser melting, the microstructure obtained for thermoforming has dendritic microstructure and fine grains. The inter-dendritic regions of Inconel 625 coatings are usually occupied by Mo, Nb rich deposits. The formation of these deposits is due to the micro-separation of these elements in the inter-dendritic regions during the solidification of the molten alloy.

Heat treatment can change the microstructure, mechanical properties and corrosion resistance by changing the temperature, storage time and cooling rate. Microstructure changes can occur with the formation of secondary phases and changes in the grain structure. Solution heat treatment and annealing can improve the mechanical properties of parts by improving grain structure and reducing residual stresses. In both SLM-HT and SLM-HT-ST samples, an increase in corrosion resistance and a decrease in the corrosion rate can be clearly seen.

Heat treatment can improve the microstructure of Inconel 625 produced by SLM and improve its mechanical properties and corrosion resistance, since the thermal process can help the precipitation of secondary phases in the alloy and protect the material against environmental factors such as high temperature and humidity.

Also, the microstructure of Inconel 625 produced by SLM after heat treatment may show a homogeneous and uniform structure, and the formation of secondary phases such as γ' (gamma prime) and carbides can increase its mechanical properties and corrosion resistance.Surface treatments such as passivation and coating can improve corrosion resistance. Surface treatments such as shot peening and electrochemical polishing can also increase the corrosion resistance of parts. In the process of shot pinning, small metal or ceramic particles are accelerated at high speed and directed to the surface of the Inconel 625 part.

The collision of particles with the surface of the part causes compressive compression in the material. Shot pinning must be carefully controlled to achieve the desired surface characteristics. Parameters such as shot size, shot speed, shot coverage, pinning time, pinning angle and pinning pressure must be carefully adjusted. Surface treatments such as mechanical polishing, chemical etching, and electrochemical treatment can improve the microstructure, mechanical properties, and corrosion resistance of Inconel 625 alloy produced by SLM. While mechanical polishing can improve the surface, this excessive treatment may deform the surface and reduce the mechanical properties. Chemical etching can remove the surface layer and create a more uniform surface. Also, electrochemical operations such as anodizing or passivation can form a protective oxide layer on the surface of Inconel 625 and increase corrosion resistance.

The microstructure of Inconel 625 produced by SLM can also be affected by various process parameters such as laser power, scan speed and powder bed temperature. In this research, the results show that surface treatment has very low effect on improving the corrosion behavior of the sample [7].

3.3. Electrochemical Impedance Spectroscopy (EIS) Test

The surface structure of different SLM electrodes has been evaluated through electrochemical impedance spectroscopy. In fact, the oxide layer was formed and its nature was analyzed through EIS. AC impedance has been used to study the metal/solution interface, oxide layers, surface treatment and corrosion behavior of organic coatings on metals. Basically, this method involves applying a low signal (10-20mV) AC to the electrochemical system and measuring the response of the system to this disturbance.When an electrochemical system is perturbed by an AC signal, the system reaches a new stable state. AC impedance is also known as electrochemical impedance spectroscopy (EIS) [8].

Drawing the virtual part of the impedance in terms of the real part is called Nyquist. This drawing is a semicircle (semicircle or arc) for each time constant. The time constant means the time it takes for the chemical composition of the electric double layer to change to a composition equivalent to the given polarization potential value. The diameter of this half circle is equivalent to corrosion resistance or coating (oxide film). If the frequency of the tip of this half-circle is measured, the capacitance value can be calculated. When the polarization is resistive, the slope of the bode-$|Z|$ curve is equal to zero, and when the capacitor is a part of the equivalent circuit, the slope of the curve is less than zero (negative).The comparison of the bode curves shows that the curvature of the phase drawing is equivalent to the level where the slope of the bode-$|Z|$ curve is negative. Also, the comparison of these two curves shows that the values of the resistances are equivalent to the frequencies of the polarized potential where the phase angle is zero [8].

EIS test in OCP potential according to Ag/AgCl (saturated KCl) electrode, in 3.5 wt.% NaCl solution and room temperature after 3600 seconds of immersion in the frequency range of 10-100 KHz with 10 mV sinusoidal potential range and 36 points was done. The obtained data were modelled using ZView software.Fig. 3., Fig. 4. and Fig. 5. show Nyquist, bode-$|Z|$ and bode-phase diagrams for different samples, respectively. As can be seen, there are two semicircles in the Nyquist diagrams and two time-constants in the bode-phase diagrams.The equivalent electric circuit model (Fig. 6.) chosen to simulate the impedance data is Rs (Rc, CPEc (RctCPEdl)).Rs includes the solution resistance measured between the reference electrode and the working electrode, the junction resistance, and the intrinsic resistance of the substrate. RC is the resistance of the outer layer (film-electrolyte interface) and CPEc is the capacitance of the coating/outer layer. Rct is the polarization resistance (charge transfer) at the interface of the substrate and the film, and CPEdl is the capacitance of the

electrical double layer of the substrate. Generally, the oxide film formed on the surface of SLM samples consists of an inner dense layer and an outer porous layer. Since the nature of the outer oxide film is porous and the surface of this oxide coating is heterogeneous, a Constant Phase Element (CPE) is used instead of an ideal capacitor in order to fit a number. When n = 1, the CPE behaves like an ideal capacitor. n is the power factor. In all the Nyquist diagrams, the collapse is observed.

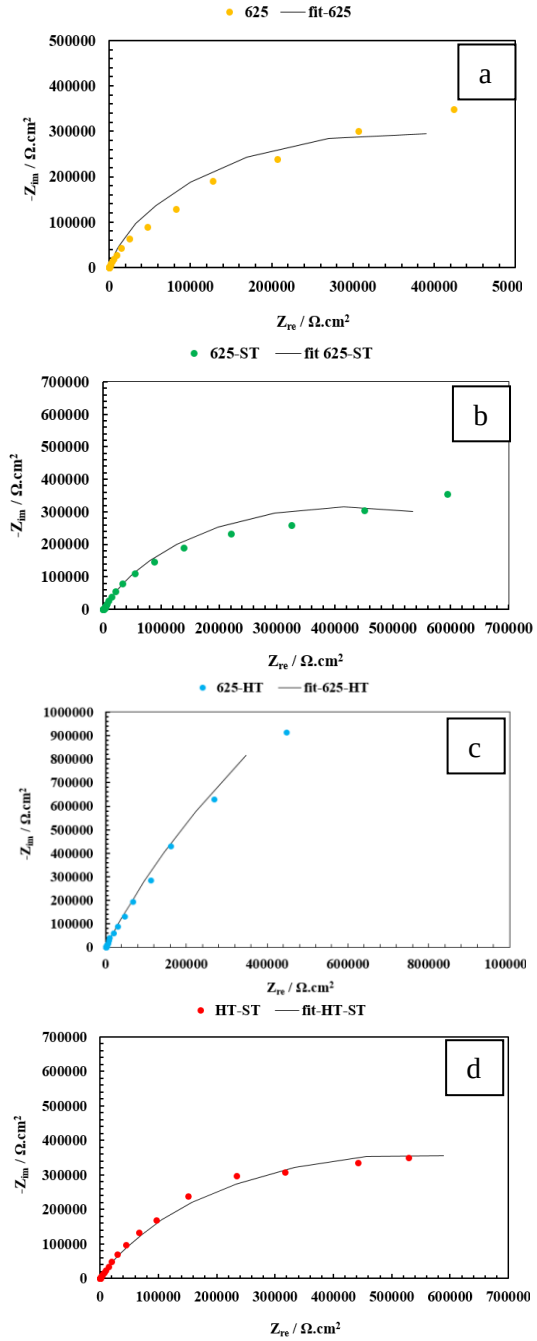

Fig. 3. Nyquist plots, a) SLM 625, b) SLM 625-ST, c) SLM 625-HT-ST and d) SLM 625-HT at OCP potential.

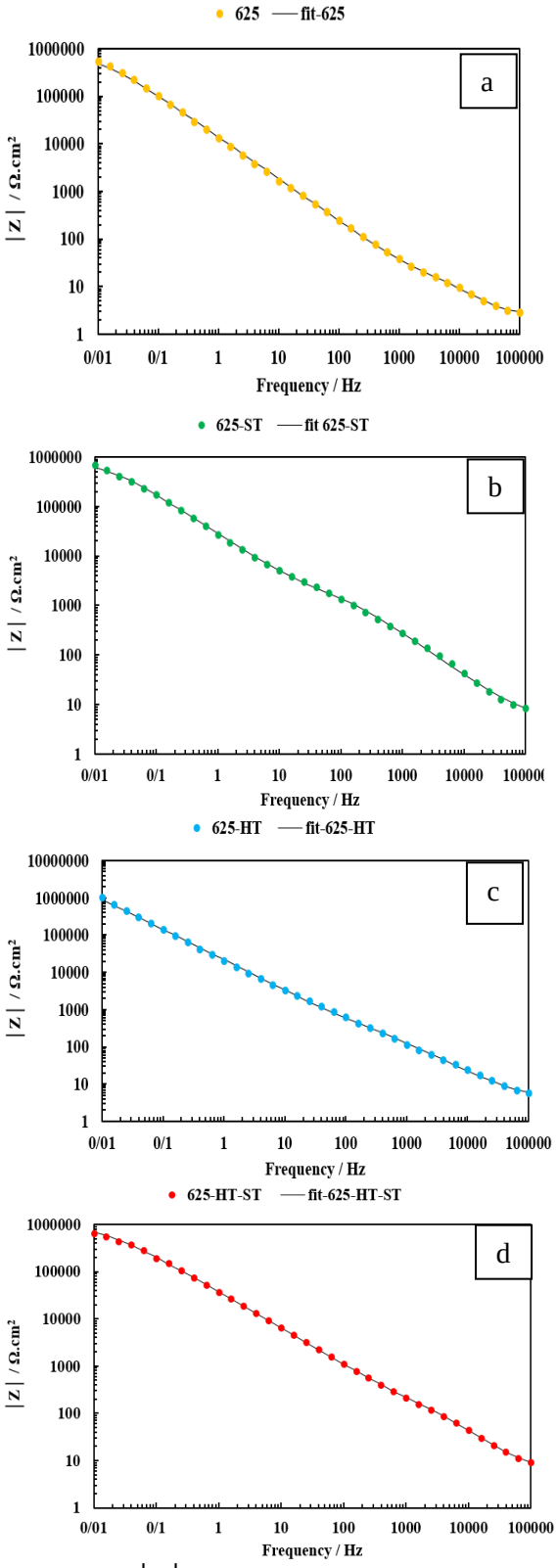

Fig. 4. Bode - |Z| diagrams, a) SLM 625, b) SLM 625-ST, c) SLM 625-HT-ST and d) SLM 625-HT at OCP potential.

Table. 2. Impedance parameters extracted from EIS test.

Sample	Rct ($\Omega.cm^2$)	n	CPEdl ($sn.\Omega^{-1}.cm^{-2}$)	Rc ($\Omega.cm^2$)	n	CPEc ($sn.\Omega$-$1.cm^{-2}$)	Rs ($\Omega.cm^2$)
625	$7.2 \times 10^{+5}$	0.86	9.8×10^{-6}	25.82	0.91	4.4×10^{-6}	3.494
625-ST	$8.5 \times 10^{+5}$	0.80	5.9×10^{-6}	2683	0.85	2.1×10^{-6}	3.727
625-HT-ST	$1.1 \times 10^{+6}$	0.73	5.6×10^{-6}	207.6	0.91	9.2×10^{-7}	3.343
625-HT	$7.8 \times 10^{+6}$	0.84	3.4×10^{-6}	968.6	0.80	6.9×10^{-6}	3.879

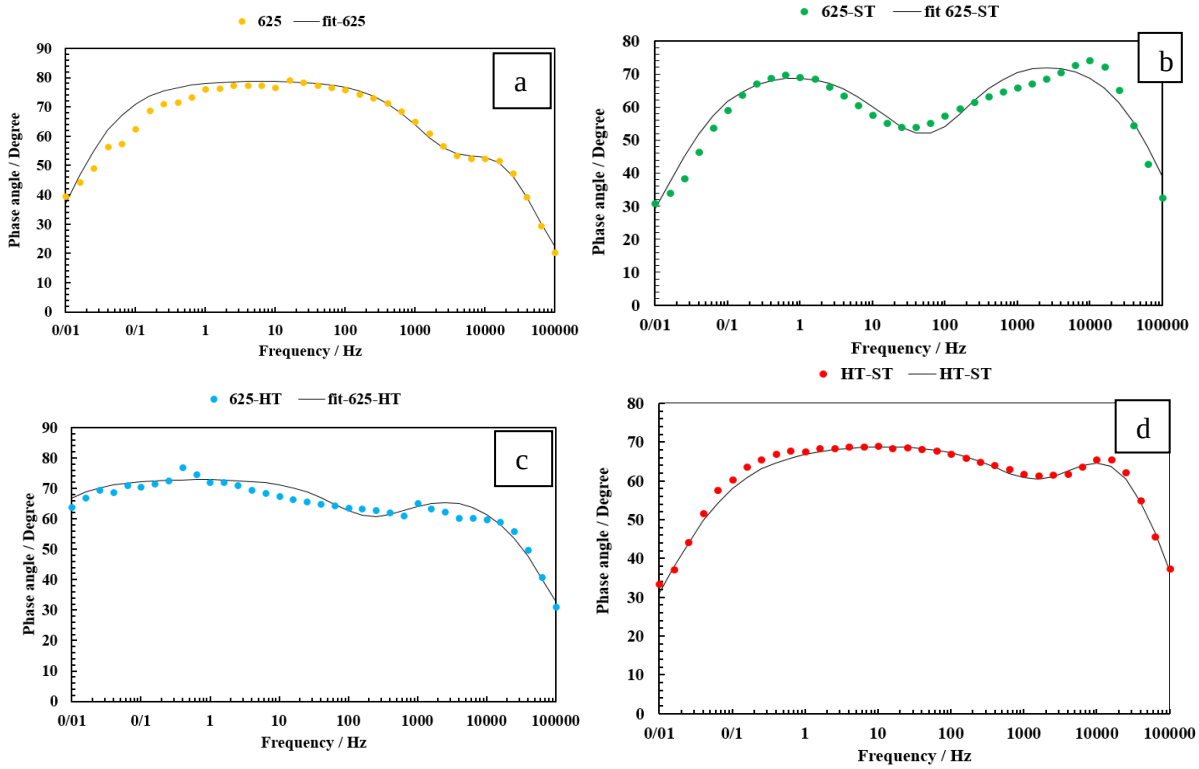

Fig. 5. Bode-phase diagrams, a) SLM 625, b) SLM 625-ST, c) SLM 625-HT-ST and d) SLM 625-HT at OCP potential.

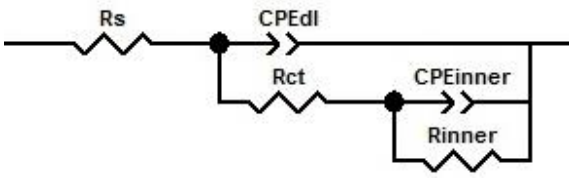

Fig. 6. Equivalent circuit model.

The impedance parameters obtained by fitting the experimental data using the equivalent electric circuit model for different samples are reported in Table. 2. As you can see, the value of solution resistance for all tests and samples is almost similar and very close to each other.It is also clear that the 625-HT sample has the highest polarization resistance and the lowest charge accumulation (capacitance), while the 625 sample shows the lowest charge transfer/polarization resistance and the highest capacitance. High load transfer resistance indicates lower corrosion rate. Again, it is clear that the heat treatment improved the corrosion resistance of the samples. Heat treatment at 1000°C followed by quenching in water (high cooling rate), maintaining Nb carbide precipitation at the grain boundary improves the corrosion performance of the alloy. While the slower the cooling rate (air or furnace cooling), the chromium carbide deposits in the alloy will reduce the corrosion characteristics of the alloy, because if chromium is involved with carbon, it is not able to form a protective layer of chromium oxide. Also, the surface treatment has led to a slight improvement in the corrosion resistance of the alloy [7].

4. Conclusion

1. SLM and SLM-ST samples have almost constant current density in high current density in a high potential range.
2. The SLM-HT sample has the most positive corrosion potential and the lowest corrosion current density, while the SLM 625 sample has the most

negative corrosion potential and the highest corrosion current density.
3. Heat treatment improves both the thermodynamic behavior and the kinetic behavior of the SLM 625 sample against corrosion.
4. In this research, the results show that surface treatment has very low effect on improving the corrosion behavior of the sample.
5. The oxide film formed on the surface of SLM samples consists of an inner dense layer and an outer porous layer, because the nature of the outer oxide film is porous and the surface of this oxide coating is heterogeneous.
6. From the results of the EIS test, it is clear that the 625-HT sample has the highest polarization resistance and the lowest charge accumulation (capacitance), while the 625 sample shows the lowest charge transfer/polarization resistance and the highest capacitance.
7. In SLM 625 and SLM 718-ST samples, primary γ phase peaks and for SLM 718-HT and SLM 718-HT-ST samples primary γ phase peaks, nickel carbide with hexagonal crystal structure and molybdenum and cubic crystal structure have been revealed.

References

[1] Cabrini M, Lorenzi S, Testa C, Pastore T, Brevi F, Biamino S, Fino P, Manfredi D, Marchese G, Calignano F, Scenini F, Evaluation of corrosion resistance of alloy 625 obtained by laser powder bed fusion. Journal of The Electrochemical Society. 2019 12;166(11):C3399.
[2] Kong D, Dong C, Ni X, Li X, Corrosion of metallic materials fabricated by selective laser melting. npj Materials Degradation. 2019 11;3(1):24.
[3] Baturina OA, Roeper DF, Olig S, Corrosion Resistance of Additively Manufactured 625 Inconel Alloy in Seawater. In Electrochemical Society Meeting Abstracts aimes 2018, 2018; 10:589-589.
[4] Lass EA, Stoudt MR, Katz MB, Williams ME, Precipitation and dissolution of δ and γ″ during heat treatment of a laser powder-bed fusion produced Ni-based superalloy. Scripta Materialia. 2018; 154:83-86.
[5] Szklarska-Smialowska Z, Pitting and crevice corrosion", NACE International, 2005.
[6] McCafferty E, Introduction to Corrosion Science. Springer; 2010.
[7] Anam MA, Microstructure and mechanical properties of selective laser melted superalloy inconel 625.
[8] Orazem ME, Tribollet B, Electrochemical impedance spectroscopy. New Jersey. 2008; 1(906):383-389.